Research Article

Global Dynamics and Numerical Simulation of a Vaccinated Mathematical Model for Rabies Disease

Hammad Jehangir[1], Nigar Ali[1], Imtiaz Ahmad[1], Hazrat Younas[1], Zubair Ahmad[2,*], Rasha F. El-Agamy[3,4]

[1]*Department of Mathematics, University of Malakand, Chakdara Dir(L), 18000, Khyber Pakhtunkhwa, Pakistan*
[2]*Dipartimento di Matematica e Fisica, Universit'a degli Studi della Campania "Luigi Vanvitelli", Caserta, Italy*
[3]*College of Computer Science and Engineering, Taibah University, Yanbu 46421, Saudi Arabia*
[4]*Computer Science Department, Faculty of Science, Tanta University, Tanta 31527, Egypt*

ABSTRACT

Rabies continues to be a major hazard to public health around the world, especially in developing countries. This article proposes an equation that describes the mechanics of animal-to-animal transmission of rabies, accounting for vaccination and infected immigrants as potential preventative strategies. The effective reproduction number (R_0) was computed using the next-generation matrix (*NGM*) Method. The Routh–Hurwitz Criterion was utilized to identify the disease-free equilibrium point (DFE). It was shown to be unstable in all other cases and to exhibit local asymptotic stability if ($R_0 < 1$). It was also found that DFE is globally asymptotically stable and quadratic Lyapunov stable. Furthermore, the normalized forward sensitivity index approach and the central manifold theory for the bifurcation analysis were used to examine the model parameters' sensitivity on the (R_0). The simulation analysis's numerical analysis comparison of RK-4 and the NSFD Method was performed using MATLAB software. A greater vaccination rate and fewer infected immigrants would delay the decline's progress, according to the simulated data's conclusions, which were visually shown.

1. INTRODUCTION

The fatal zoonotic virus that causes rabies is mostly spread to humans and other animals through the bites or scratches of infected animals like skunks, dogs, foxes, raccoons, and bats. The virus, found mainly in the saliva of these animals, enters the bloodstream and travels via the peripheral nerve system to the brain, or through neuromuscular junctions after replicating in the muscles. Upon reaching the brain, Rabies causes acute inflammation, leading to coma and, ultimately, death. The disease has the highest case fatality rate of any infectious disease, approaching 100% once clinical symptoms appear [1, 2].

The primary human source of rabies is dogs, responsible for the vast majority of cases worldwide. Transmission occurs through bites, scratches, or contact with saliva on mucosal surfaces like the eyes, nose, or mouth. While Rabies can also be transmitted through organ transplants or aerosol exposure, such instances are exceedingly rare. Early symptoms of Rabies mimic those of the flu, including fever, pain at the site of the bite, and unusual sensations. As the central nervous system becomes infected, it leads to severe brain inflammation, causing hyperactivity, paralysis, and death [3].

Following a bite, the location and intensity of the bite, the quantity of virus delivered, and the promptness of post-exposure prophylaxis (PEP) all affect the chance of contracting rabies. The likelihood of contracting rabies following a bite in the

absence of PEP to the head is about 55%, while bites to the limbs carry a lower risk. Rabies transmission through rodents is very uncommon, and Transmission from person to person is quite uncommon with only a few documented cases occurring through tissue and organ transplants [4].

The incubation period for Rabies in humans typically ranges from 1 to 3 months but can vary from as short as 7 days to over a year, depending on the bite's location and intensity, the quantity of virus injected, and additional host variables. In comparison to bites on the extremities, bites on the face, neck, and hands have a higher risk and a shorter incubation period because they are closer to the brain. The incubation time in dogs is about 3 to 8 weeks but can extend up to 6 months in rare cases. Despite the high fatality rate, a few cases of human survival have been documented, mostly involving post-exposure vaccination or specialized treatment protocols like the Milwaukee protocol. However, survival has been more common in cases involving bat strains of the virus, whereas canine strains are generally more virulent [5].

Rabies remains a significant public health concern, particularly in Africa and Asia, where the majority of cases occur, especially in children under 15. In these regions, dog-mediated transmission is to blame for up to 99% of occurrences of rabies in humans. Poverty, lack of awareness, and inadequate healthcare infrastructure contribute to the high mortality rates in these areas. However, Rabies elimination is possible with widespread dog vaccination initiatives, which have proven effective in reducing transmission in various settings worldwide [5, 6].

Mass vaccination of dogs is the primary strategy for controlling Rabies, effectively interrupting transmission between canines and lowering the danger to people. The chance of contracting rabies from other sources, such as wildlife, is increasing as the prevalence of rabies caused by dogs decreases. Wild carnivores and bats are significant reservoirs for the virus, posing a higher risk for transmission [7].

Various mathematical models have been developed to study Rabies transmission dynamics and evaluate control strategies. These models have shown that vaccination is the most effective method for controlling the disease, while culling is less effective. Some models also consider the impact of time delays between infection and infectiousness, demonstrating that such delays can significantly affect the mechanics of the spread of rabies and the effectiveness of control measures [8].

In summary, Rabies is a nearly universally fatal disease with significant public health implications, particularly in regions with inadequate vaccination coverage and healthcare infrastructure. Mass vaccination campaigns targeting dogs are crucial for controlling and ultimately eliminating the disease, with mathematical models providing valuable insights into the most effective strategies for Rabies control [9].

2. MODEL FORMULATION

$$\begin{cases} \frac{S_h}{dt} = A_h + \alpha_2 V_h - (\alpha_1 + \mu_h + \beta_{dh} I_h) S_h, \\ \frac{E_h}{dt} = \beta_{dh} S_h I_h - (\alpha_h + \delta_h + \mu_h) E_h, \\ \frac{I_h}{dt} = \alpha_h E_h - (\mu_h + m_h) I_h, \\ \frac{V_h}{dt} = \alpha_1 S_h - (\alpha_2 + \mu_h) V_h, \\ \frac{R_h}{dt} = \delta_h E_h - \mu_h R_h, \\ \frac{S_d}{dt} = B_d + \rho_d V_d - (c_d + \mu_d + \beta_{dd} I_d) S_d, \\ \frac{I_d}{dt} = \beta_{dd} S_d I_d - (\mu_d + m_d) I_d, \\ \frac{V_d}{dt} = c_d S_d - (\mu_d + \rho_d) V_d, \end{cases} \qquad (1)$$

Graphically it can be seen in Fig. 1, while the Initial conditions are given below:
$S_h(0) > 0, \quad E_h(0) \geq 0, \quad I_h(0) \geq 0, \quad V_h(0) \geq 0, \quad R_h(0) \geq 0, \quad S_d(0) \geq 0, \quad I_d(0) \geq 0. V_d(0) \geq 0,$
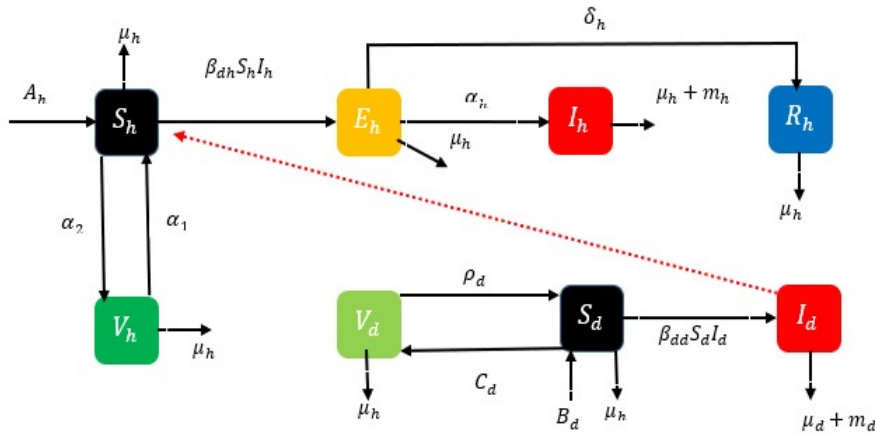
Fig. 1. Flow-chart of the proposed Model

Parameters	Humans	Dogs
Recruitment Rate	A_h: The recruitment rate of susceptible humans (e.g., birth rate or immigration).	B_d: The recruitment rate of susceptible dogs (e.g., dog birth rate).
Vaccination Rate	α_1: The rate at which susceptible humans are vaccinated.	c_d: The rate at which susceptible dogs are vaccinated or treated.
Immunity Loss Rate	α_2: The rate at which vaccinated humans lose immunity and become susceptible again.	ρ_d: The rate at which vaccinated dogs lose immunity and become susceptible again.
Transmission Rate	β_{dh}: The transmission rate of the disease from the vector (e.g., mosquitoes) to humans.	-
Natural Death Rate	μ_h: The natural death rate of humans.	μ_d: The natural death rate of dogs.
Infectious Progression	δ_h: The rate at which exposed humans become infectious.	-
Disease-Induced Mortality	m_h: The disease-induced mortality rate in humans.	m_d: The disease-induced mortality rate in dogs.
Infectious Progression Rate	α_h: The rate at which exposed humans become infectious.	-
Vector Transmission Rate	β_{dd}: The transmission rate of the disease from infected vectors to susceptible vectors.	-

TABLE I. Parameters for Humans and Dogs

3. MODEL ANALYSIS

We shall study model system (1) in the following biologically viable area. Model system (1) is essentially split into two areas, such $\Omega = \Omega_h \times \Omega_d$, [10]

Lemma 1. *the solution set $\{S_h, E_h, I_h V_h, R_h, S_d, I_d, V_d\} \in R_+^8$ of Model system (1), is contained in the feasible region Ω,*

Proof. Suppose $\{S_h, E_h, I_h V_h, R_h, S_d, I_d, V_d\} \in R_+^8$ for every $t > 0$. In order to examine the dynamics of model system (1), we aim to demonstrate that the area Ω is positively invariant.

$$N_h(t) = S_h(t) + E_h(t) + I_h(t) + V_h(t) + R_h(t), \tag{2}$$

$$N_h(t) = S_d(t) + I_d(t) + V_d(t), \tag{3}$$

where $N_d(t)$ represents the total dog population at any given moment. N_h and (t) represent the entire human population at any given period. (t) Formula (2) gives

$$\frac{N_h(t)}{dt} = A_h - (\mu_h S_h + \mu_h E_h + \mu_h I_h + \mu_h R) - m_h I_h \tag{4}$$

$$\frac{N_h(t)}{dt} = A_h - (N_h(t) - m_h I_h \tag{5}$$

Similarly 3 gives

$$\frac{N_d(t)}{dt} = B_d - (\mu_d S_d + +\mu_d I_d + \mu_d V) - m_d I_d \tag{6}$$

$$\frac{N_d(t)}{dt} = B_d - (N_d(t) - m_h I_d \tag{7}$$

Now, assuming that the dogs' compartment is free of disease-induced mortality rates and culling effects, it follows that 6 and 7 become

$$\frac{N_h(t)}{dt} = A_h - m_h N - h \tag{8}$$

$$\frac{N_d(t)}{dt} = B_d - m_d(N_d(t), \tag{9}$$

Suppose $\frac{N_h(t)}{dt} \geq 0, \frac{N_d(t)}{dt} \geq 0, N_h \geq \frac{A_h}{m_h}$ and $N_d \geq \frac{B_d}{m_d} \geq \frac{B_d}{m_d}$, and after that using the theorem put forth in[32] on differential inequality results in $0 \geq N_h \geq \frac{A_h}{m_h}$ and $0 \geq N_d \geq \frac{N_d}{m_d}$ 8 and 9

$$\frac{N_h(t)}{dt} \geq A_h - m_h N - h \tag{10}$$

$$\frac{N_d(t)}{dt} \geq B_d - m_d(N_d(t), \tag{11}$$

Solve 10 and 11 using the IF (integrating factor) approach. Hence, $I.F = e^{\int p(t)dt}$ and $\frac{dy}{dt} + p(t)y = Q$. The region is the possible solution for the dogs population in model system (1) after some algebraic modification.

$$\Omega_d = \{(S_d, I_d, V_d) \in R_+^3, N_d \geq \frac{B_d}{m_d}\} \tag{12}$$

In a similar manner, the human population does as well. According to 11, this suggests that the human population of model system (1) may be solved in the area

$$\Omega_h = \{(S_h, E_h, I_h, V_h, R_h) \in R_+^5, N_h \geq \frac{A_h}{m_d}\} \tag{13}$$

Therefore, Ω contains the workable solutions. $\Omega = \Omega_h \times \Omega_d$, as a result, It follows from the common comparison theorem on differential inequality

$$N_h \geq N_h(0)e^{-(m_h)t} + \frac{A_h}{m_h}\left(1 - e^{-(m_h)t}\right) \tag{14}$$

$$N_d \geq N_d(0)e^{-(m_d)t} + \frac{B_d}{m_d}\left(1 - e^{-(m_d)t}\right) \tag{15}$$

Hence, the total dog population size $N_d(t)$ as $t \to \infty$ approaches $\frac{D_d}{m_d}$. Similarly, as $t \to \infty$, the size of the human population as a whole $N_h(t)$ approaches $\frac{A_h}{m_h}$. This means that as time approaches infinity, the infected state variables

$(S_h, E_h, I_h,$ and $V_h)$ of the two populations trend to zero. Consequently, all of the solutions in $\mathbb{R}^8_+$ are being drawn to or attracted by the area Ω, which results in the set of workable solutions for model system (1) as described in [10].

$$
\begin{pmatrix} S_h \\ E_h \\ I_h \\ V_h \\ R_h \\ S_d \\ I_d \\ V_d \end{pmatrix} \in R^8_+ \Big| \begin{pmatrix} S_h \geq 0 \\ E_h \geq 0 \\ I_h \geq 0 \\ V_h \geq 0 \\ R_h \geq 0 \\ S_d \geq 0 \\ I_d \geq 0 \\ V_d \geq 0 \\ N_h \geq \frac{A_h}{m_h} \\ N_d \geq \frac{B_d}{m_d} \end{pmatrix} \tag{16}
$$

Hence, (1) is mathematically well-posed and epidemiologically meaningful.

4. BASIC QUALITATIVE PROPERTIES OF THE MODEL(1)

The rabies Model is significant both mathematically and physiologically if and only if each state variable in the model is non-negative bounded in the invariant zone.

$$
\Omega = \{(S_h, E_h, I_h, V_h, R_h,) \in R^5_+, \quad N_h \geq \left(\frac{(\alpha_2 + \mu_h)A_h}{(\alpha_1\alpha_2 - (\alpha_2 + \mu_h))} \right)
$$
$$
S_d, I_d, V_d \in R^3_+, \quad N_d \geq \left(\frac{\alpha_1(\alpha_2 + \mu_h)A_h}{(\alpha_1\alpha_2 - (\alpha_2 + \mu_h))(\alpha_2 + \mu_h)} \right)\} \tag{17}
$$

Theorem 4.1. *(Positivity of the model solutions) Let us give the initial data in equation (condition no) then the solution $S_h(t), E_h(t), I_h(t), V_h(t),$*
$R_h(t), S_d(t), I_d(t), V_d(t)$ of the Model (1), are non-negative for all time $t > 0$, [11]

Proof. Let us consider $S_h(0) > 0, E_h(0) > 0, I_h(0) > 0, V_h(0) > 0, R_h(0) > 0, S_d(0) > 0, I_d(0) > 0, V_d(0) > 0$ then for all time $t > 0$, we have to show that $S_h(0) > 0, E_h(0) > 0, I_h(0) > 0, V_h(0) > 0, R_h(0) > 0, S_d(0) > 0, I_d(0) > 0, V_d(0) > 0$. Define $\Pi = Sup\{S_h(0) > 0, E_h(0) > 0, I_h(0) > 0, V_h(0) > 0, R_h(0) > 0, S_d(0) > 0, I_d(0) > 0, V_d(0) > 0\}$. We may now argue that $\Pi > 0$, if $\Pi = +\infty$, then non-negativity exists given that every state variable in the rabies model (1) is continuous and positive. However, if $0 < \Pi < +\infty$, then $S(\Pi) = 0, S_h(\Pi) > 0, E_h(\Pi) > 0, I_h(\Pi) > 0, V_h(\Pi) > 0, R_h(\Pi) > 0, S_d(\Pi) > 0, I_d(\Pi) > 0, V_d(\Pi) > 0$ from the first equation of the model (1) we get

$$
S(\Pi) = M_1 S(0) + M_1 \int_0^\Pi exp^{\int_0^\Pi (\alpha_2 + \mu_h + \beta_{dh})dt} (A_h + \alpha_2) \, dt > 0,
$$

where

$$
M_1 = exp^{-(\mu_h t + \int_0^\Pi \alpha_2 + \beta_{dh} > 0}, S(0) > 0.
$$

and from the meaning of Π the solution $S_h(t) > 0, E_h(t) > 0, I_h(t) > 0, V_h(t) > 0, R_h(t) > 0, S_d(t) > 0, 2, V_d(t) > 0, I_d(t) > 0$ Moreover, since the exponential function is always positive, $S(\Pi) \neq 0$. hence the solution $S(\Pi) > 0$. Thus, all of model (1)'s solutions are non-negative after applying the same process for $\Pi = +\infty$.

5. DISEASE FREE EQUILIBRIUM POINT (DFE)

This can only be accomplished if there is no RABV infection in the population, which implies that there are no humans who have been treated, recovered, or infected by diseased dogs—that is, $(E_h^0 = I_h^0 = R_h^0 = I_d^0 = 0)$. After model equations (1) are found, the RABV free equilibrium is provided by (F^0)

$$
F^0 = (S_h^0, E_h^0, I_h^0, V_h^0, R_h^0, S_d^0, I_d^0, V_d^0,) \tag{18}
$$

$$
F^0 = \left(\frac{(\alpha_2 + \mu_h)A_h}{\alpha_2\alpha_h + (\alpha_2 + \mu_h)^2}, 0, 0, \frac{(\alpha_2 + \mu_h)^2 A_h - A_h(\alpha_h\alpha_2 + (\alpha_2 + \mu_h)^2)}{\alpha_h(\alpha_2\alpha_h + (\alpha_2 + \mu_h)^2)}, 0, \frac{(\mu_d + \rho_d)B_d}{(\mu_d + \rho_d)(c_d + \mu_d)}, 0, \frac{c_d(\mu_d + \rho_d)B_d}{(\mu_d + \rho_d)^2(c_d + \mu_d)} \right)
$$
$$
\tag{19}
$$

6. BASIC REPRODUCTIVE NUMBER R_0

The Basic Reproductive Number in epidemiology, or R_0, is a crucial idea, used to measure the transmission potential of an infectious condition. It displays the average number of secondary infections that an infected individual within a susceptible group produces. In other words, it quantifies the ability of a disease to spread within a population. If $R_0 > 1$, each existing infection is causing more than one new infection, indicating that the disease is likely to spread within the population. If $R_0 < 1$, each existing infection is causing less than one new infection, suggesting that the disease will likely die out in the population over time. Now we use the *NGM* Method to the R_0 as follow [1, 9]

$$\begin{cases} \frac{E_h}{dt} = \beta_{dh}S_h I_h - (\alpha_h + \delta_h + \mu_h)E_h, \\ \frac{I_h}{dt} = \alpha_h E_h - (\mu_h + m_h)I_h, \\ \frac{I_d}{dt} = \beta_{dd}S_d I_d - (\mu_d + m_d)I_d, \end{cases} \tag{20}$$

$$F = \begin{pmatrix} \beta_{dh}S_h I_d \\ 0 \\ \beta_{dd}S_d I_d \end{pmatrix}, \quad F^* = \begin{pmatrix} 0 & 0 & \beta_{dh}S_h^0 \\ 0 & 0 & 0 \\ 0 & 0 & \beta_{dd}S_d^0 \end{pmatrix},$$

$$V = \begin{pmatrix} (\alpha_h + \delta_h + \mu_h)E_h \\ (\mu_h + m_h)I_h - \alpha_h E_h \\ (\mu_d + m_d)I_d \end{pmatrix}$$

$$V^* = \begin{pmatrix} (\alpha_h + \delta_h + \mu_h) & 0 & 0 \\ -\alpha_h & (\mu_h + m_h) & 0 \\ 0 & 0 & (\mu_d + m_d) \end{pmatrix}$$

$$V^{-1} = \begin{pmatrix} \frac{1}{\alpha_h+\delta_h+\mu_h} & 0 & 0 \\ \frac{\alpha_h m_d + e_h + e_h \alpha_h \mu_d}{(m_d+\mu_d)(m_d+\mu_d)(\alpha_h+\delta_h+\mu_h)} & \frac{1}{m_d+\mu_d} & 0 \\ 0 & 0 & \frac{1}{m_d+\mu_d} \end{pmatrix}$$

$$F^*V^{-1} = \begin{pmatrix} 0 & 0 & \frac{\beta_d h S_h^0}{m_d+\mu_d} \\ 0 & 0 & 0 \\ 0 & 0 & \frac{\beta_{dd}S^0}{(m_d+\mu_d)} \end{pmatrix}$$

$$R_0 = \frac{\beta_{dd}}{(m_d+\mu_d)}\left(\frac{c_d(\mu_d+\rho_d)B_d}{(\mu_d+\rho_d)^2(c_d+\mu_d)}\right) \tag{21}$$

7. LOCAL STABILITY OF DISEASE FREE EQUILIBRIUM POINT

Theorem 7.1. *In set B, at the disease-free equilibrium F_0, the suggested system (1) is considered local asymptotically stable (LAS) if $R_0 < 1$, and unstable if $R_0 > 1$[10].*

Proof.

$$JE_0 = \begin{pmatrix} -(\alpha_1+\mu_h) & 0 & 0 & \alpha_2 & 0 & 0 & \beta_d h S_h^* & 0 \\ 0 & -c_1 & 0 & 0 & 0 & 0 & \beta_d h S_h^* & 0 \\ 0 & \alpha_h & -c_2 & 0 & 0 & 0 & 0 & 0 \\ \alpha_1 & 0 & 0 & -c_3 & 0 & 0 & 0 & 0 \\ 0 & \delta_h & 0 & 0 & -\mu_h & 0 & 0 & 0 \\ 0 & 0 & 0 & 0 & 0 & -(c_d+\mu_d) & \beta_{dd}S^* & \rho_d \\ 0 & 0 & 0 & 0 & 0 & 0 & -(\mu_d+m_d) & 0 \\ 0 & 0 & 0 & 0 & 0 & c_d & 0 & -(\mu_d+\rho_d) \end{pmatrix} \tag{22}$$

where, $c_1 = (\alpha_h + \delta_h + \mu)$, $c_2 = (\mu_h + m_h)$, $c_3 = (\alpha_2 + \mu_h)$ $\lambda_1 = -(\alpha_1 + \mu_h)$, $\lambda_2 = -(\alpha_h + \delta_h + \mu_h)$ the compounding eigenvalue of the of the above system is given, $\lambda_1 = -(\alpha_1 + \mu_h) < 0$, since $\alpha_1 + \mu_h) > 0$ and $\lambda_2 = -(\alpha_h + \delta_h + \mu_h) < 0$, since $(\alpha_h + \delta_h + \mu_h) > 0$, $\lambda_3 = -(\alpha_h + \delta_h + \mu_h)(\mu_h + m_h) < 0$, since $(\alpha_h + \delta_h + \mu_h)(\mu_h + m_h) > 0$ $\lambda_4 = -(\alpha_1\alpha_2 - (\alpha_2 + \mu_h)^2) < 0$, since $(\alpha_1\alpha_2 - (\alpha_2 + \mu_h)^2) > 0$ $\lambda_5 = -\mu_h(\alpha_h + \delta_h + \mu_h) < 0$, since $\lambda_5 = -\mu_h(\alpha_h + \delta_h + \mu_h) > 0$, $\lambda_6 = -(c_d + \mu_d)c_d < 0$, since $(c_d + \mu_d)c_d < 0$, $\lambda_7 = -(\mu_d + m_d) < 0$, $(\mu_d + m_d) > 0$ $\lambda_8 = -(c_d\rho_d(\mu_d + \delta_d)(c_d + \mu_d)) < 0$, since $(c_d\rho_d(\mu_d + \delta_d)(c_d + \mu_d)) > 0$ all the eigenvalues are negative, therefore the disease is free of rabies since there are no human cases of the disease. There is no infection in the host population, and the human population as a whole is in good health. Additionally, the F_0 is unstable if $R_0 > 1$. $R_0 > 1$,

7.1 Global Stability of the Disease-free Equilibrium

The Castillo-Chavez et al. [11] method is used to examine the equilibrium devoid of disease's worldwide stability. Subsequently, the model system (1) might be stated as follows:

$$
\begin{cases}
\frac{dP}{dt} = F(P, Q), \\
\frac{dQ}{dt} = G(P, 0), G(P, 0) = 0.
\end{cases}
\tag{23}
$$

Theorem 7.2. *Where $P \in R^m$ represents the disease-free equilibrium point, $Q \in R^n$, the number of infected compartments, and the number of uninfected compartments, $E^0 = (P^0, 0)$. In order to ensure the global asymptotic stability of DEF, it is necessary to meet the conditions (H_1) and (H_2) below. The point of equilibrium for the disease free, $E_0 = (P^0, 0)$, is globally asymptotically stable if $R_0 < 1$, and unstable if otherwise [12]*

Proof. : The rabies model (1) can written as, $p = (S_h, V_h, R_h, S_d, V_d)$, $Q = (E_h, I_h, I_d)$, and
$E_0 = \{ \frac{(\alpha_2+\mu_h)A_h}{\alpha_2\alpha_h+(\alpha_2+\mu_h)^2}, 0, 0, \frac{(\alpha_2+\mu_h)^2 A_h - A_h(\alpha_h\alpha_2+(\alpha_2+\mu_h)^2)}{\alpha_h(\alpha_2\alpha_h+)(\alpha_2+\mu_h)^2}, 0, \frac{(\mu_d+\rho_d)B_d}{(\mu_d+\rho_d)(c_d+\mu_d)}, 0, \frac{c_d(\mu_d+\rho_d)B_d}{(\mu_d+\rho_d)^2(c_d+\mu_d)} \}$.
Now we have

$$
\frac{dP}{dt} =
\begin{pmatrix}
A_h + \alpha_2 V - (\alpha_2 + \mu_h + \beta_{dh}I_d)S_h \\
\alpha_1 S_h - (\alpha_2 + \mu_h)V_h \\
\delta_h E_h - \mu_h R_h \\
B_d + \rho_d V_d - (c_d + \mu_d + \beta_{dd}I_d)S_h \\
c_d S_d - (\mu_d + \rho_d)
\end{pmatrix}
\tag{24}
$$

At disease free equilibrium point we get

$$
\frac{dP}{dt} = (P^0, 0) =
\begin{pmatrix}
A_h + \alpha_2 \frac{(\alpha_2+\mu_h)^2 A_h - A_h(\alpha_h\alpha_2+(\alpha_2+\mu_h)^2)}{\alpha_h(\alpha_2\alpha_h+)(\alpha_2+\mu_h)^2} - (\alpha_2 + \mu_h + \beta_{dh}I_d)\frac{(\alpha_2+\mu_h)A_h}{\alpha_2\alpha_h+(\alpha_2+\mu_h)^2} \\
\alpha_1 \frac{(\alpha_2+\mu_h)A_h}{\alpha_2\alpha_h+(\alpha_2+\mu_h)^2} - (\alpha_2 + \mu_h)A_h + \alpha_2 \frac{(\alpha_2+\mu_h)^2 A_h - A_h(\alpha_h\alpha_2+(\alpha_2+\mu_h)^2)}{\alpha_h(\alpha_2\alpha_h+)(\alpha_2+\mu_h)^2} \\
0 \\
B_d + \rho_d A_h + \alpha_2 \frac{(\alpha_2+\mu_h)^2 A_h - A_h(\alpha_h\alpha_2+(\alpha_2+\mu_h)^2)}{\alpha_h(\alpha_2\alpha_h+)(\alpha_2+\mu_h)^2} - (c_d + \mu_d + \beta_{dd}I_d)\frac{(\alpha_2+\mu_h)A_h}{\alpha_2\alpha_h+(\alpha_2+\mu_h)^2} \\
c_d \frac{(\alpha_2+\mu_h)A_h}{\alpha_2\alpha_h+(\alpha_2+\mu_h)^2} - (\mu_d + \rho_d)
\end{pmatrix}
\tag{25}
$$

$F(P^0, 0)$ has a unique equilibrium point
$\left[\frac{(\alpha_2+\mu_h)A_h}{\alpha_2\alpha_h+(\alpha_2+\mu_h)^2}, \frac{(\alpha_2+\mu_h)^2 A_h - A_h(\alpha_h\alpha_2+(\alpha_2+\mu_h)^2)}{\alpha_h(\alpha_2\alpha_h+)(\alpha_2+\mu_h)^2}, \frac{(\mu_d+\rho_d)B_d}{(\mu_d+\rho_d)(c_d+\mu_d)}, \frac{c_d(\mu_d+\rho_d)B_d}{(\mu_d+\rho_d)^2(c_d+\mu_d)} \right]$. This is globally asymptotically stable; hence, the second condition's condition (H_1), holds. (H_2),

$$
G(P, Q) =
\begin{pmatrix}
\beta_{dh}S_h I_d - (\alpha_h + \delta_h + \mu_h)E_h \\
\alpha_h E_h - (\mu_h + m_h)I_h \\
\beta_{dd}S_d I_d - (\mu_d + m_d)
\end{pmatrix}
\tag{26}
$$

Then we get

$$
X = A_1(P^0, 0) =
\begin{pmatrix}
-(\alpha_h + \delta_h + \mu_h) & 0\beta_{dh}S_h^0 & \\
\alpha_h & -(\mu_h + m_h) & 0 \\
0 & 0 & \beta_{dd}S_d^0
\end{pmatrix}
\tag{27}
$$

Now that the off-diagonal elements of the matrix X are non-negative, it is evident that the matrix is a matrix. $G^-(P, Q) = XA - G(P, Q)$ equals to

$$
G^-(P, Q) =
\begin{pmatrix}
-(\alpha_h + \delta_h + \mu_h) & 0 & \beta_{dh}S_h^0 \\
\alpha_h & -(\mu_h + m_h) & 0 \\
0 & 0 & \beta_{dd}S_d^0
\end{pmatrix}
\begin{pmatrix} E_h \\ I_h \\ I_d \end{pmatrix}
\begin{pmatrix}
\beta_{dh}S_h I_d - (\alpha_h + \delta_h + \mu_h)E_h \\
\alpha_h E_h - (\mu_h + m_h)I_h \\
\beta_{dd}S_d I_d - (\mu_d + m_d)
\end{pmatrix}
\tag{28}
$$

$$
G^-(P, Q) =
\begin{pmatrix}
\beta_{dh}S_h^0 - (\alpha_h + \delta_h + \mu_h) \\
0 \\
\beta_{dd}S_d^0 - (\mu_d + m_d)V_d^0
\end{pmatrix}
\tag{29}
$$

. Since it clear that $S_h^0 > S_h$ and $V_h^0 > V_h$, and $S_d^0 > S_d$, and $V_d^0 > V_d$, Consequently, it is evident that $G^-(P, Q) \geq 0$, and $P^0 = (S_h^0, V_h^0, S_d^0 . V_d^0)$ is globally asymptotically stable,

8. ENDEMIC EQUILIBRIUM POINT

A second equilibrium solution derived by solving the system of algebraic equations represents the case where $I \neq 0$. This approach is known as the "endemic equilibrium solution" and looks like this:[9]

$$\begin{cases} S_h^* = \frac{A_h + \alpha_2 V^*}{(\alpha_2 + \mu_h + \beta_{dh} I_d^*)}, \\ E_h^* = \frac{\beta_{dh} S_h^* I_d^*}{(\alpha_h + \delta_h + \mu_h)}, \\ I_H^* = \frac{\alpha_h E_h}{(\mu_h + m_h) I_h^*}, \\ V_h^* = \frac{\alpha_1 S_h^*}{(\alpha_2 + \mu_h)}, \\ R_h^* = \frac{\delta_h E *_h}{\mu_h R_h^*}, \\ S_d^* = \frac{B_d + \rho_d V_d^*}{(c_d + \mu_d + \beta_{dd} I_d^*)}, \\ I_d^* = \frac{\beta_{dd} S_d^* I_d^*}{(\mu_d + m_d)}, \\ V_d^* = \frac{c_d S_d^*}{(\mu_d + \rho_d)}, \end{cases} \tag{30}$$

8.1 Global Stability of the Endemic Equilibrium Point

The global stability of the endemic equilibrium point B^0 was established using the Lyapunov function developed by Vargas-De-León [13], and it was further studied. The Lyapunov function $V(x)$ is said to be asymptotically globally stable at the point where it occurs if $\frac{dV}{dt} < 0$.

Theorem 8.1. *The rabies epidemic in the Model System has a unique endemic equilibrium point B^*, which is unstable otherwise and globally asymptotically stable if $R_0 > 1$.[14]*

Proof. Examining the quadratic Lyapunov function by itself

$$V(y_1, y_2, y_3, ..., y_n) = \sum_{i=1}^{n} \frac{1}{2} \left[y_i - y_i^* \right]^2,$$

where y^* is the endemic equilibrium point and y_i is the population of the *ith* compartment. The following is a positive definite function for the model system 1.

$$V(S_h, \ E_h, \ I_h, \ V_h, \ R_h, \ S_d, \ I_d, \ V_d) = \sum_{i=1}^{n} \frac{1}{2} \left[y_i - y_i^* \right]^2, \tag{31}$$

The rabies model system's Lyapunov function is thus expressed as follows:

$$V = \frac{1}{2} [(S_h - S_h^*) + (E_h - E_h^*) + (I_h - I_h^*) + (V_h - V_h^*) + (R_h - R_h^*) + (S_d - S_d^*) + (I - I_d^*) + (V - V_d^*)]^2, \tag{32}$$

Clearly $V : R_+^8 \to R$ is a differentiable, continuous function. Next, the function $V(t)$ can be differentiated with respect to time to obtain:

$\frac{dV}{dt} = [(S_h - S_h^*) + (E_h - E_h^*) + (I_h - I_h^*) + (V_h - V_h^*) + (R_h - R_h^*) + (S_d - S_d^*) + (I - I_d^*) + (V - V_d^*)]$
$\frac{d}{dt}(S_h + E_h + I_h + V_h + R_h + S_d + I_d + V_d)$

$$\Rightarrow \frac{dN}{dt}(S_h + E_h + I_h + V_h + R_h + S_d + I_d + V_d) = A_h - \mu_h(N_h(t)) - m_h I_h - N_d(t) - m_d I_d + B_d -$$

$$(S_h^* + E_h^* + I_h^* + V_h^* + R_h^*) = \frac{A_h + m_h}{\mu_h}, (S_d^* + I_d^* + V_d^*) = \frac{B_d - \mu_d}{\mu_d}, \tag{33}$$

$$\frac{dV_h}{dt} = \left[N_h(t) - \frac{A_h - m_h I_h^*}{\mu_h} \right] \left[N_h(t) - \frac{A_h - m_h I_h^*}{\mu_h} \right] \tag{34}$$

$$\frac{dV_h}{dt} = -\left[N_h(t) - \frac{A_h - m_h I_h^*}{\mu_h} \right]^2 \tag{35}$$

$$\frac{dV_d}{dt} = -\left[N_d(t) - \frac{B_d - m_d I_d^*}{\mu_d} \right]^2 \tag{36}$$

Since $\frac{dV_{h,d}}{dt} < 0$ is evident, it follows that B^0, the Endemic Equilibrium Point, is asymptotically stable worldwide.

9. NUMERICAL SIMULATION

This section's numerical simulation was carried out with the aid of MATLAB2016a software and the ODE solver that combines the applications of Runge-Kutta (RK4) and RK5, fourth and fifth order algorithms. When it comes to modeling the dynamics of the rabies transmission model, it has proven to be quite accurate. The beginning circumstances are assumed to be random in sequence to produce a certain model behavior. The population dynamics of the rabies population are shown in Fig. 2. The results demonstrate that throughout the early years, the proportion of sensitive animals rapidly decreased. The illness contracted by interacting with diseased animals and the decline in vulnerable animals are the main causes of this decline. Animals that are sensitive are less susceptible to contracting the virus when they come into contact with infected individuals.
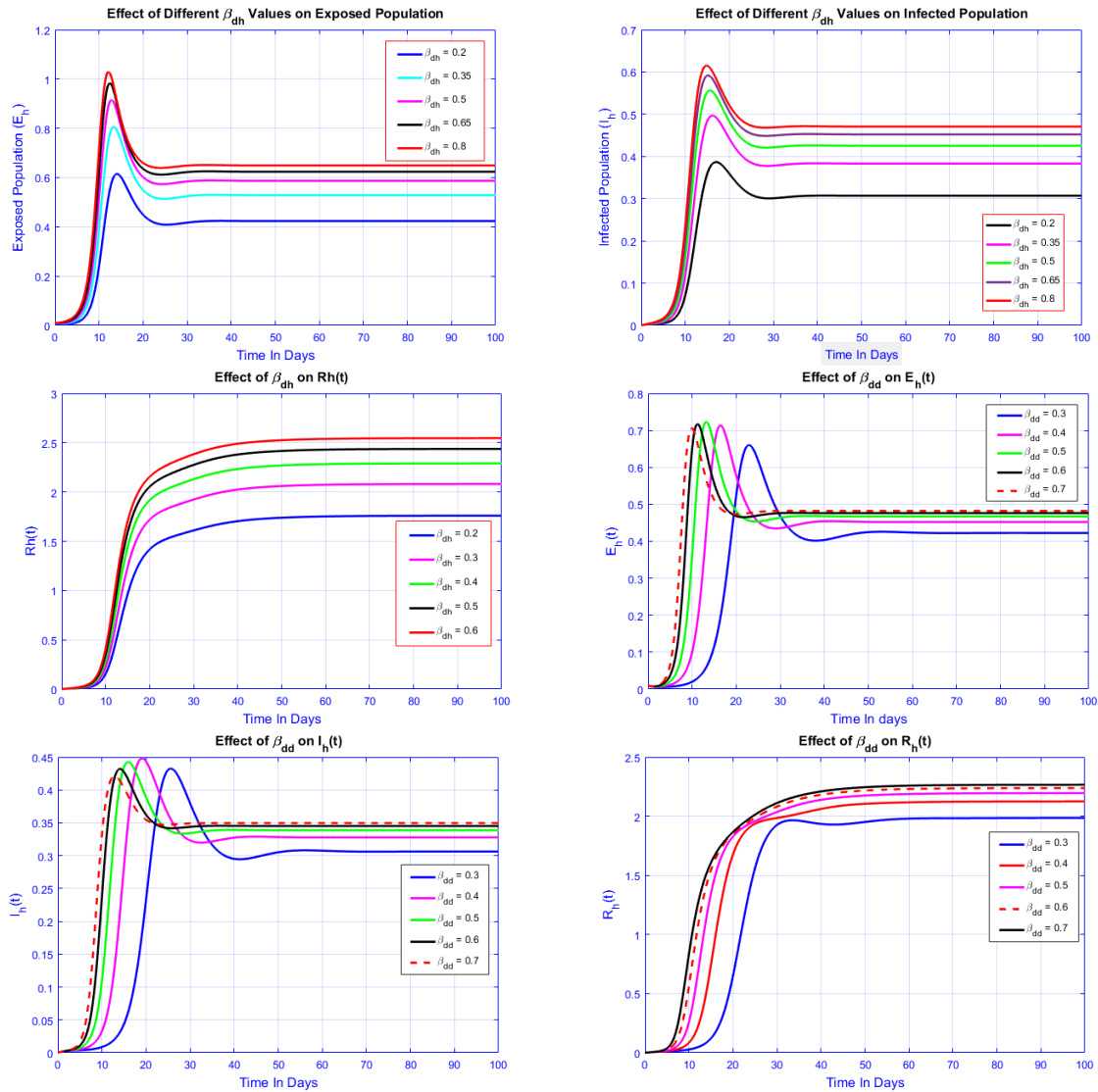
Fig. 2. Population dynamics of the rabies population

Regarding small β_{dh} values (such as $\beta_{dh} = 0.1$): Slow population decline in the susceptible group suggests a decreased rate of transmission. The number of vulnerable individuals gradually decreases as a result of the disease's less effective spread. For large levels of β_{dh} (such as $\beta_{dh} = 0.5$), This suggests a faster rate of transmission. The item As a result, the illness spreads more quickly. As more people become exposed and sick, the number of susceptibles rapidly declines. The dynamics of disease propagation may be understood by examining the impact of various β_{dh} values on the exposed population (E). This analysis reveals that the transmission rate is quite significant. Higher β_{dh} values produce a quick increase in the number of exposed persons, resulting in a faster and more extensive epidemic, whereas lower β_{dh} β_{dd} and values cause the illness to spread more slowly. This emphasizes how crucial it is to use treatments meant to lower the rate

of transmission in order to manage and lessen the effects of infectious illnesses. These results underscore the importance of interventions aimed at reducing the transmission rate β_{dh} to control and mitigate the impact of infectious diseases in Figures 4 and 3, Measures such as vaccination, social distancing, wearing masks, and improving hygiene can effectively lower β_{dh} thereby reducing the spread of the disease. By maintaining a lower β_{dh}, it is possible to prevent a rapid and overwhelming outbreak, allowing for better management of healthcare resources and minimizing the overall impact on the population.
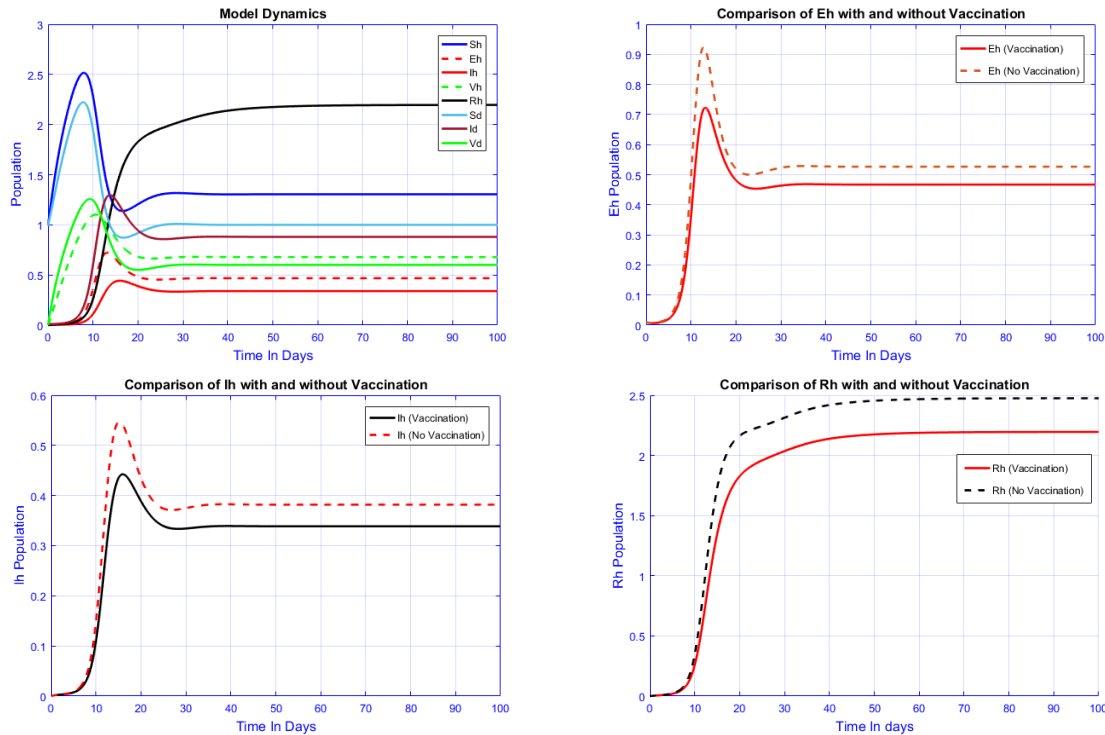

Fig. 3. Comparison of model dynamics for vaccinated and non-vaccinated populations

Effect of Vaccination: The vaccination procedure results in a notable decrease in the vulnerable population, according to the vaccination scenario see Fig. 3, and see Fig. 4, fewer people are vulnerable and because vaccinations are administered directly to individuals, the exposed and infected populations are often smaller in vaccination scenarios. In the vaccination scenario, there is a higher percentage of recovered persons, suggesting that vaccination contributes to a greater number of recovery cases. The vaccinated compartment, which is exclusive to the vaccination scenario, illustrates how vaccination might lower the populations of exposed and infected individuals. These findings demonstrate the value of vaccination in halting the spread of infectious illnesses by lowering the proportion of vulnerable and contagious people, which eventually results in fewer cases and a speedier rate of population recovery. For example, $\alpha_1 = 0.13$ and $\alpha_2 = 0.15$ are the values of the parameters α_1 and α_2 that correspond to the vaccination scenario. These metrics stand for vaccination rates among the vulnerable population and vaccine efficiency, respectively. Both α_1 and α_2 are 0 in the case of no immunization. This indicates that there is no vaccination and that the system operates as though there are no vaccination effects.

10. NUMERICAL ANALYSIS

The numerical interpretation of model (1) using RK4 and the Matlab-coded NSFD approach is the main topic of this section. As table 1 shows, a variety of parameters together with their respective numerical values have been collected from [2, 4]. Initially, we create the two epidemic model numerical approaches. Next, using the graphs, we can monitor the dynamic behavior of MODEL (1) over time t by numerical simulations. We also talk about the numerical outcomes.

10.1 RK4 Scheme

In order to formulate an explicit numerical scheme for the RK4 approach [15-18], the following presumptions must be made. $S_h(t) \approx S_h^n, E_h(t) \approx E_h^n, I_h(t) \approx I_h^n, V_h(t) \approx V_h^n, R_h(t) \approx R_h^n, S_d(t) \approx S_d^n, I_d(t) \approx I_d^n, V_d(t) \approx V_d^n$

$$k_1 = h\left[A_h + \alpha_2 V_h^n - (\alpha_1 + \mu_h + \beta_{dh}I_d^n)S_h^n\right],$$

$$w_1 = h\left[\beta_{dh}S_h^n I_d^n - (\alpha_h + \delta_h + \mu_h)E_h^n\right],$$

$$m_1 = h\left[\alpha_1 S_h^n - (\alpha_2 + \mu_h)V_h^n,\right],$$

$$n_1 = h\left[\delta_h E_h^n - \mu_h R_h^n,\right],$$

$$o_1 = h\left[B_d + \rho_d V_d^n - (c_d + \mu_d + \beta_{dd}I_d^n)S_d^n\right],$$

$$p_1 = h\left[\beta_{dd}S_d^n I_d^n - (\mu_d + m_d)I_d^n,\right],$$

$$q_1 = h\left[\beta_{dd}S_d^n I_d^n - (\mu_d + m_d)I_d^n\right],$$

$$v_1 = h\left[c_d S_d^n - (\mu_d + \rho_d)V_d^n\right],$$

$$k_2 = h\left[A_h + \alpha_2 \left(V_h^n \frac{n_1}{2}\right) - \left(\alpha_1 + \mu_h + \beta_{dh}\left(I_d^n + \frac{q_1}{2}\right)(S_h^n + \frac{k_1}{2})\right)\right],$$

$$w_2 = h\left[\beta_{dh}\left(S_h^n + \frac{k_1}{2}\right)\left(I_d^n + \frac{q_1}{2}\right) - (\alpha_h + \delta_h + \mu_h)\left(E_h^n + \frac{w_1}{2}\right)\right],$$

$$m_2 = h\left[\alpha_1 \left(S_h^n + \frac{k_1}{2}\right) - (\alpha_2 + \mu_h)\left(V_h^n + \frac{n_1}{2}\right)\right],$$

$$n_2 = h\left[\alpha_1 \left(S_h^n + \frac{k_1}{2}\right) - (\alpha_2 + \mu_h)\left(V_h^n + \frac{n_1}{2}\right)\right]$$

$$o_2 = h\left[\delta_h \left(E_h^n + \frac{w_1}{2}\right) - \mu_h \left(R_h^n + \frac{o_1}{2}\right)\right],$$

$$p_2 = h\left[B_d + \rho_d \left(V_d^n + \frac{n_1}{2}\right) - (c_d + \mu_d + \beta_{dd}\left(I_d^n + \frac{q_1}{2}\right)S_d^n + \frac{p_1}{2})\right],$$

$$q_2 = h\left[\beta_{dd}\left((S_d^n + \frac{p_1}{2})(I_d^n + \frac{q_1}{2})\right) - (\mu_d + m_d)I_d^n,\right],$$

$$v_2 = h\left[c_d \left(S_d^n + \frac{p_1}{2}\right) - (\mu_d + \rho_d)\left(V_d^n + \frac{v_1}{2}\right)\right],$$

Hence

$$S_h^{n+1} = S_h^n + \frac{1}{16}\left[k_1 + 2k_2 + 2k_3 + 2k_4 + 2k_4 + 2k_5 + 2k_6 + k_7 + k_8\right] \tag{37}$$

$$E_h^{n+1} = E_h^n + \frac{1}{16}\left[w_1 + 2w_2 + 2w_3 + 2w_4 + 2w_4 + 2w_5 + 2w_6 + 2w_7 + w_8\right] \tag{38}$$

$$I_h^{n+1} = I_h^n + \frac{1}{16}\left[m_1 + 2m_2 + 2m_3 + 2m_4 + 2m_4 + 2m_5 + 2m_6 + 2m_7 + m_8\right] \tag{39}$$

$$V_h^{n+1} = I_h^n + \frac{1}{16}\left[n_1 + 2n_2 + 2n_3 + 2n_4 + 2n_4 + 2n_5 + 2n_6 + 2n_7 + n_8\right] \tag{40}$$

$$R_h^{n+1} = R_h^n + \frac{1}{16}\left[o_1 + 2o_2 + 2o_3 + 2o_4 + 2o_4 + 2o_5 + 2o_6 + 2o_7 + o_8\right] \tag{41}$$

$$S_d^{n+1} = E_d^n + \frac{1}{16}\left[p_1 + 2p_2 + 2p_3 + 2p_4 + 2p_4 + 2p_5 + 2p_6 + 2p_7 + p_8\right] \tag{42}$$

$$I_d^{n+1} = I_d^n + \frac{1}{16}\left[q_1 + 2q_2 + 2q_3 + 2q_4 + 2q_4 + 2q_5 + 2q_6 + 2q_7 + q_8\right] \tag{43}$$

$$V_d^{n+1} = V_d^n + \frac{1}{16}\left[j_1 + 2j_2 + 2j_3 + 2j_4 + 2j_4 + 2j_5 + 2j_6 + 2j_7 + j_8\right] \tag{44}$$

10.2 NSFD schemne

We introduce a trustworthy numerical method in this subsection, which is based on the Mickens created the non-standard finite difference (NSFD) methodology [19]. This methodology finds several uses in the examination of numerous real-world, practical issues that crop up in the engineering and mathematics disciplines. We refer to [20, 21] for NSFD technique applications in various applied mathematics domains. In order to provide the following in model (1) based on the first equation in order to create an explicit numerical scheme for the NSFD method.

$$\frac{S_h}{dt} = \frac{S_h^{n+1} - S_h}{h}, S_h(t) \approx S_h^{n+1}, I_h(t)S_h(t) = I_h^n S_h^{n+1}$$

from the 2nd equation of the model (1),

$$\frac{E_h}{dt} = \frac{E_h^{n+1} - E_h}{h}, E_h(t) \approx E_h^{n+1}, I_h(t)S_h(t) = I_h^n S_h^{n+1}$$

from the 3rd equation of the model (1),

$$\frac{I_h}{dt} = \frac{I_h^{n+1} - I_h}{h}, I_h(t) \approx I_h^{n+1},$$

from the 4th equation of the model (1), let

$$\frac{V_h}{dt} = \frac{V_h^{n+1} - V_h}{h}, V_h(t) \approx V_h^{n+1}, E_h(t) = E_h^n$$

from the 5th equation of the model (1), let

$$\frac{R_h}{dt} = \frac{R_h^{n+1} - R_h}{h}, R_h(t) \approx R_h^{n+1},$$

from the 6Th equation of the model (1),

$$\frac{S_d}{dt} = \frac{S_d^{n+1} - S_d}{h}, S_d(t) \approx S_d^{n+1}, I_d(t)S_d(t) = I_d^n S_d^{n+1}$$

from the 7Th equation of the model (1),

$$\frac{I_d}{dt} = \frac{I_d^{n+1} - I_d}{h}, I_d(t) \approx E_d^{n+1}, E_d(t) = E_d^n$$

from the 8Th equation of the model (1), let

$$\frac{V_d}{dt} = \frac{V_d^{n+1} - V_d}{h}, V_h(t) \approx V_d^{n+1},$$

using the above assumption the eight equation of the model (1), become, Thus,

$$S_h^{n+1} = \frac{S_h^n + h(A_h + \alpha_2 V_h^n)}{1 + h(\alpha_2 + \mu_h + \beta_{dh} I_d^n)} \tag{45}$$

$$E_h^{n+1} = \frac{E_h^n + h(\beta_{dh} I_h^n S_h^n)}{(1 + h(\alpha_h + \delta_h + \mu_h)} \tag{46}$$

$$I_h^{n+1} = \frac{I_h^n + h(\mu_h + m_h}{(1 + h(\alpha_2 + \mu_h)} \tag{47}$$

$$V_h^{n+1} = \frac{V_h^n + h(\alpha_1 S_h^n + V_h^n)}{1 + (\alpha_2 + \mu_h)} \tag{48}$$

$$R_h^{n+1} = \frac{R_h^n + \delta_h E_h^n}{1 + h(\mu_h)}, \tag{49}$$

$$S_d^{n+1} = \frac{S_d^n + h(S^d \beta_d + \rho_d V_d^n)}{1 + h(c_d + \mu_d + \beta_{dd} I_d^n)} \tag{50}$$

$$I_d^{n+1} = \frac{I_d^n + h(\beta_{dd} S_d^n + I_d^n}{1 + h(\mu_d + m_d)} \tag{51}$$

$$V_d^{n+1} = \frac{V_d^n + h(c_d S_d^n + V_d^n)}{1 + h(\mu_d + \rho_d)} \tag{52}$$

Theorem 10.1. *The continuous model (1)'s equilibrium points (E_0 and E_1, respectively) are preserved by the discrete scheme (29)–(35). In other words, the continuous model's endemic equilibrium, also known as the disease-free equilibrium point (1) are the only fixed points in scheme (29)–(35). Furthermore, the NSFD scheme's equilibrium points and fixed points have the same stability properties.*

10.3 Numerical Results

The numerical interpretation of model (1) utilizing the Matlab-coded RK4 (21)–(28) and NSFD is presented in this section technique (29)–(35). Initially, we compare the h = 1.0 discretization step size for the RK4 and NSFD approaches. Both numerical methods are numerically Figs. 2-3 demonstrate that they are convergent and converge to the real steady states (E_0 and E_1) of the continuous model (1), respectively. Furthermore, RK4 and NSFD offer excellent solutions for h = 1.0 in the fundamental feasible region B. Crucially, for $R_0 < 1$, the RK4 approach produces positive solutions if we pick h = 1.5, moving away from the genuine steady state and converges to the true steady state of E_0. On the other hand, for $R_0 > l$, it wanders away from the genuine steady state and does not converge to E_1, leading to unanticipated negative solutions that are never found inside set B. In contrast, the NSFD method yields positive solutions and converges to both E_0 and E_1 when $R_0 < 1$.
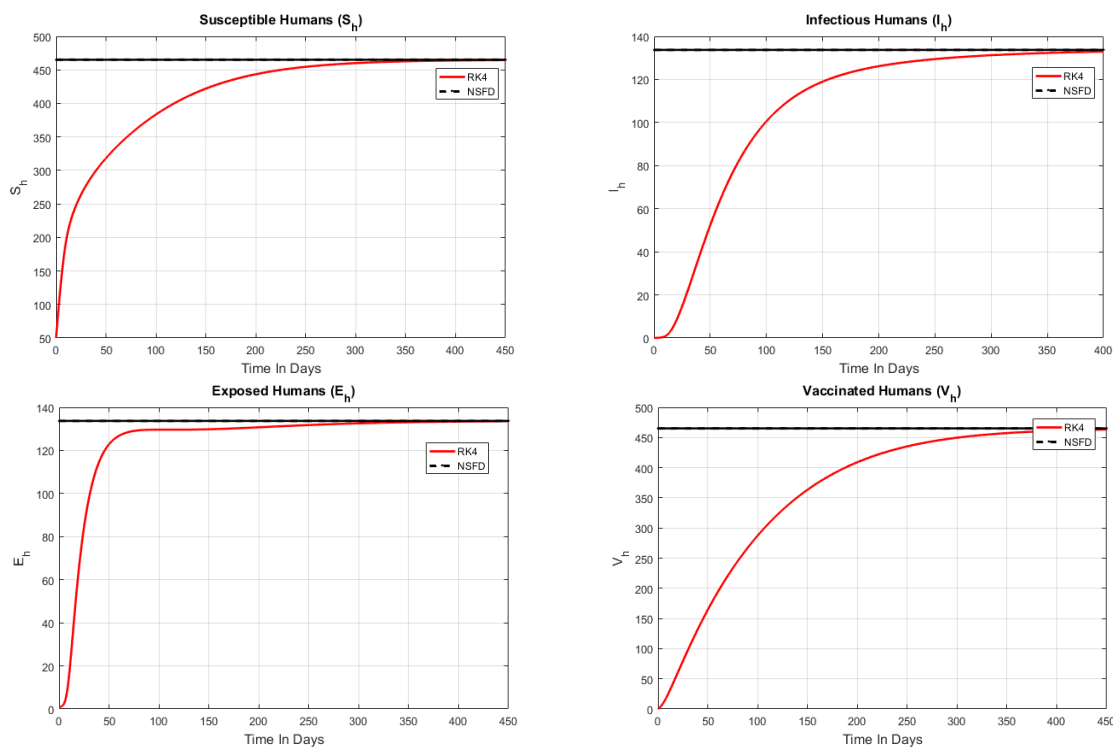

Fig. 4. Comparison of population dynamics using NSFD and RK4

Although extremely large or very tiny time steps may still have an impact on accuracy and stability, the approach is typically stable over a wide range of time steps. The code supplied selects a time step of $dt = 0.01$, which strikes a compromise between computing efficiency and precision.

Susceptible Humans (S_h) : A comprehensive trajectory of susceptible humans across time will be provided by the RK4 approach. Depending on the settings, you may see variations in the amount of people that are vulnerable due to things like recovery and illness transmission rates. Other Variables: In a similar vein, the dynamics outlined by the model equations will cause variables such as exposed individuals (E_h), infected humans (I_h), and recovered humans (R_h), to alter. Some of the shortcomings of conventional techniques, such as RK4, are intended to be addressed by the Numerically Stable Finite Difference (NSFD) method, particularly with regard to stability and the treatment of stiff equations. Although the NSFD implementation's specifications aren't disclosed, the following is what to generally anticipate: Stability: Where standard approaches such as Euler or RK4 may struggle, NSFD methods prove especially helpful for stiff systems. Even with longer time periods, they can maintain stability and manage quick changes in variables more effectively. Accuracy: Although NSFD techniques are stable, their accuracy may not always match that of RK4, particularly if the discretization

scheme is less sophisticated. They make up for it, nonetheless, with increased stability in rigid systems. RK4 is a fantastic choice. It's well-established, accurate, and extensively used in numerous applications. If you have unique demands relating to stability or other features, NSFD would be worth studying further, but it requires careful implementation.

Conflicts of Interest

The authors declare no conflicts of interest.

Funding

Acknowledgment

REFERENCES

[1]   Hayman, D. T., Johnson, N., Horton, D. L., Hedge, J., Wakeley, P. R., Banyard, A. C., & Fooks, A. R. (2011). Evolutionary history of rabies in Ghana. *PLOS Neglected Tropical Diseases, 5*(4), e1001.

[2]   Kotola, B. S., Teklu, S. W., & Abebaw, Y. F. (2023). Bifurcation and optimal control analysis of HIV/AIDS and COVID-19 co-infection model with numerical simulation. *Plos one, 18*(5), e0284759.

[3]   Castillo-Chavez, C., & Song, B. (2004). Dynamical models of tuberculosis and their applications. *Mathematical Biosciences & Engineering, 1*(2), 361-404.

[4]   Chauhan, S. (2020). Comprehensive review of coronavirus disease 2019 (COVID-19). *Biomedical journal, 43*(4), 334-340.

[5]   Qasim Gilani, S., Syed, T., Umair, M., & Marques, O. (2023). Skin cancer classification using deep spiking neural network. *Journal of Digital Imaging, 36*(3), 1137-1147.

[6]   Savov, P., Jatowt, A., & Nielek, R. (2020). Identifying breakthrough scientific papers. *Information Processing & Management, 57*(2), 102168.

[7]   Lempp, C., Jungwirth, N., Grilo, M. L., Reckendorf, A., Ulrich, A., Van Neer, A., & Siebert, U. (2017). Pathological findings in the red fox (Vulpes vulpes), stone marten (Martes foina) and raccoon dog (Nyctereutes procyonoides), with special emphasis on infectious and zoonotic agents in Northern Germany. *PLoS One, 12*(4), e0175469.

[8]   Hankins, D. G., & Rosekrans, J. A. (2004). Overview, prevention, and treatment of rabies. *Mayo Clinic Proceedings, 79*(5), 671-676.

[9]   Fisher, C. R., Streicker, D. G., & Schnell, M. J. (2018). The spread and evolution of rabies virus: conquering new frontiers. *Nature Reviews Microbiology, 16*(4), 241-255.

[10] Demirci, E. (2014). A new mathematical approach for Rabies endemy. *Applied Mathematical Sciences, 8*(2), 59-67.

[11] Castillo-Chavez, C. (2002). On the computation of R0 and its role on global stability. In *Mathematical approaches for emerging and reemerging infectious diseases: an introduction* (Vol. 1, p. 229).

[12] Qasim Gilani, S., Syed, T., Umair, M., & Marques, O. (2023). Skin cancer classification using deep spiking neural network. *Journal of Digital Imaging, 36*(3), 1137-1147.

[13] Vargas-De-Leon, C. (2009). Constructions of Lyapunov functions for classic SIS, SIR and SIRS epidemic models with variable population size. *Foro-Red-Mat: Revista electronica de contenido matematico, 26*(5), 1-12.

[14] Balaha, H. M., & Hassan, A. E. S. (2023). Skin cancer diagnosis based on deep transfer learning and sparrow search algorithm. *Neural Computing and Applications, 35*(1), 815-853.

[15] Simon, C., Davidsen, K., & Hansen, C. (2019). A text mining tool for performing classification of biomedical literature. *Bioinformatics, 57*(1), 165-170.

[16] Kalathil, N., Byrnes, J. J., Randazzese, L., Hartnett, D. P., & Freyman, C. A. (2018). Application of text analytics to extract and analyze material–application pairs from a large scientific corpus. *Frontiers in Research Metrics and Analytics, 2*, 15.

[17] Blei, D. M., Ng, A. Y., & Jordan, M. I. (2003). Latent Dirichlet allocation. *Journal of Machine Learning Research, 3*(Jan), 993-1022.

[18] Gan, J., & Qi, Y. (2021). Selection of the optimal number of topics for LDA topic model—taking patent policy analysis as an example. *Entropy, 23*(10), 1301.

[19] Lushasi, K., Hayes, S., Ferguson, E. A., Changalucha, J., Cleaveland, S., Govella, N. J., & Hampson, K. (2021). Reservoir dynamics of rabies in south-east Tanzania and the roles of cross-species transmission and domestic dog vaccination. *Journal of Applied Ecology, 58*(11), 2673-2685.

[20] Khan, I. U., Mustafa, S., Shokri, A., Li, S., Akgül, A., & Bariq, A. (2023). The stability analysis of a nonlinear mathematical model for typhoid fever disease. *Scientific Reports, 13*(1), 15284.

[21] Lushasi, K., Hayes, S., Ferguson, E. A., Changalucha, J., Cleaveland, S., Govella, N. J., & Hampson, K. (2021). Reservoir dynamics of rabies in south-east Tanzania and the roles of cross-species transmission and domestic dog vaccination. *Journal of Applied Ecology, 58*(11), 2673-2685.